Supplementary Information

Importance of dynamic lattice effects for crystal field excitations in quantum spin ice candidate $Pr_2Zr_2O_7$.

Y. Xu, H. Man, N. Tang, S. Baidya, H. Zhang, S. Nakatsuji, D. Vanderbilt, and N. Drichko

(Dated: July 20, 2021)

I. EXPERIMENTAL

Raman spectra were measured using the Jobin-Yvon T64000 triple monochromator spectrometer equipped with a liquid nitrogen cooled CCD detector. Raman scattering was excited with 514.5 nm of Ar^+-Kr^+ laser. Raman spectra were measured in the temperature range from 300 to 6 K, and in the frequency range from 3.7 to 125 meV with spectral resolution 0.125 meV. The spectral regions below and above 18.6 cm^{-1} were measured using the triple-monochromator and single-c options, respectively. Both micro and macro Raman setups were used in this work. Micro-Raman spectra were measured using a standard Olympus microscope attached to the spectrometer in backscattering geometry with laser power density 0.32 $mW/\mu m^2$. Macro-Raman spectra were measured using the pseudo-Brewster's angle geometry with laser power density 0.0013 $mW/\mu m^2$. All spectra were normalized by the Bose-Einstein thermal factor.

For the measurement, the electric field vector of the excitation laser light $\hat{e}_l$ and of the scattered light $\hat{e}_s$ were oriented along x and y directions ($x \perp y$) in the (111) crystallographic plane. Crystal structure of $Pr_2Zr_2O_7$ is of $Fd\bar{3}m$ (No. 227) space group, which corresponds to O_h point group. In Tab. I we present what symmetries of scattering channels are observed in the two measured geometries.

TABLE I: Components of Raman tensor for (x, x) and (x, y) polarizations.

Geometry	A_{1g}	E_g	T_{2g}
(x, x)	a^2	b^2	c^2
(x, y)	0	b^2	$\frac{2}{3}c^2$

Spectra were fitted with a sum of Lorentzian line shapes. Also fitted by Gaussian-Lorentzian sum, which shows that their width is defined by the lifetime of the excitations. The fits provide the positions and line widths of the CEF excitations as discussed below.

II. FULL RANGE RAMAN SPECTRA
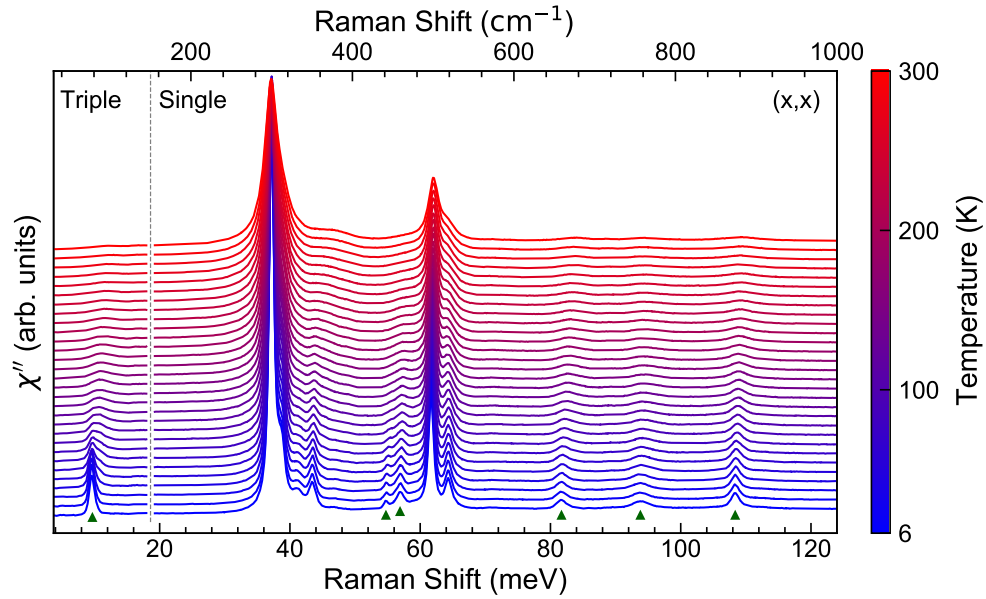
FIG. 1: Temperature dependence of the macro-Raman spectra of $Pr_2Zr_2O_7$ from 6 to 300 K in parallel polarization configuration (x, x). CEF excitations are marked by green triangles.
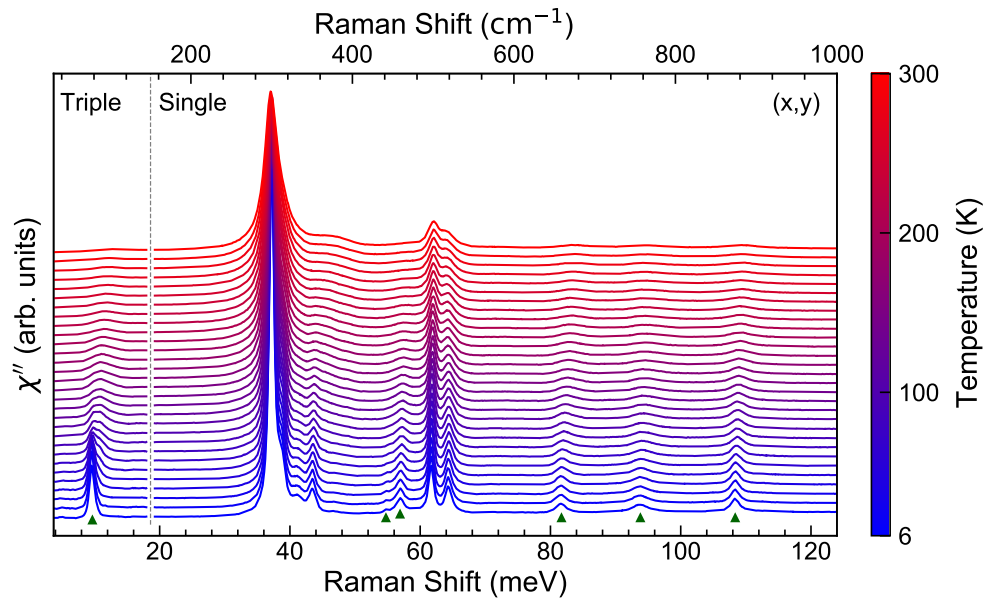
FIG. 2: Temperature dependence of the macro-Raman spectra of $Pr_2Zr_2O_7$ from 6 to 300 K in parallel polarization configuration (x, y). CEF excitations are marked by green triangles.
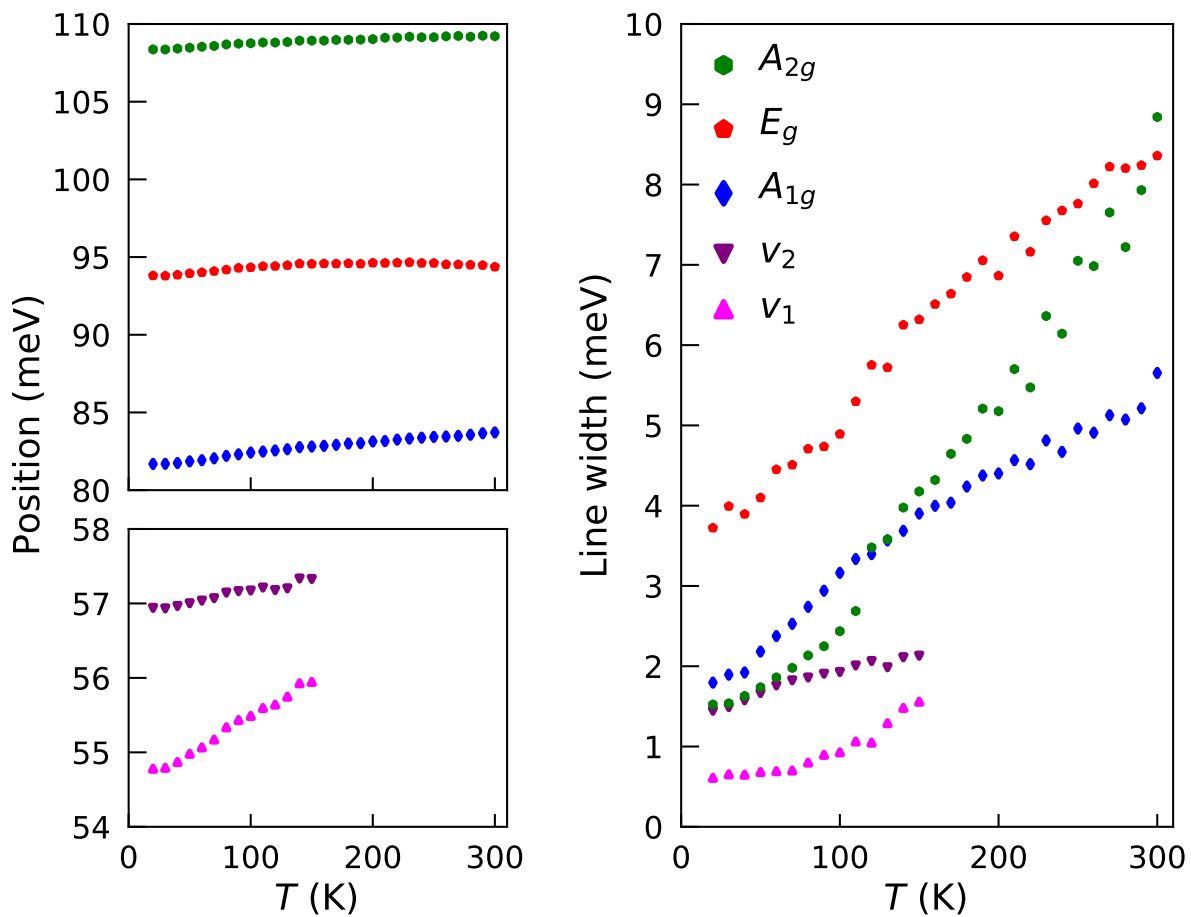
FIG. 3: Temperature dependence of the positions and the line widths of the vibronic states and the CEF states.

III.   SPECTRAL FITTING METHODS

The spectra in main text Fig. 2a were fitted by a sum of the Lorentzian function given by

$$L(x) = \frac{a}{1 + (\frac{x-\omega}{\Gamma/2})^2},$$ (1)

where a is the height of the peak, ω is the position of the maximum, and Γ is the full width at half maximum.

The spectra in Fig. 3a were fitted by a sum of the Gaussian-Lorentzian (pseudo-Voigt) function given by

$$f(x) = \eta \frac{1}{2} G(x) + (1 - \eta)L(x) = \eta e^{-\ln 2(\frac{x-\omega}{\Gamma/2})^2} + (1 - \eta)\frac{a}{1 + (\frac{x-\omega}{\Gamma/2})^2},$$ (2)

where η is the mixing parameter, a is the height of the peak, ω is the position of the maximum, and Γ is the full width at half maximum.

Fig. 4 presents the results of Gaussian-Lorentzian fits for the $E_g^0 \rightarrow A_{1g}$ transition. From 14 K to 40 K, the spectra are mostly dominated by the blue component. From 45 K to 100 K, the spectra are well described two distinct Gaussian-Lorentzian peaks. Above 100 K, two components merge into a broad peak and become undistinguishable.
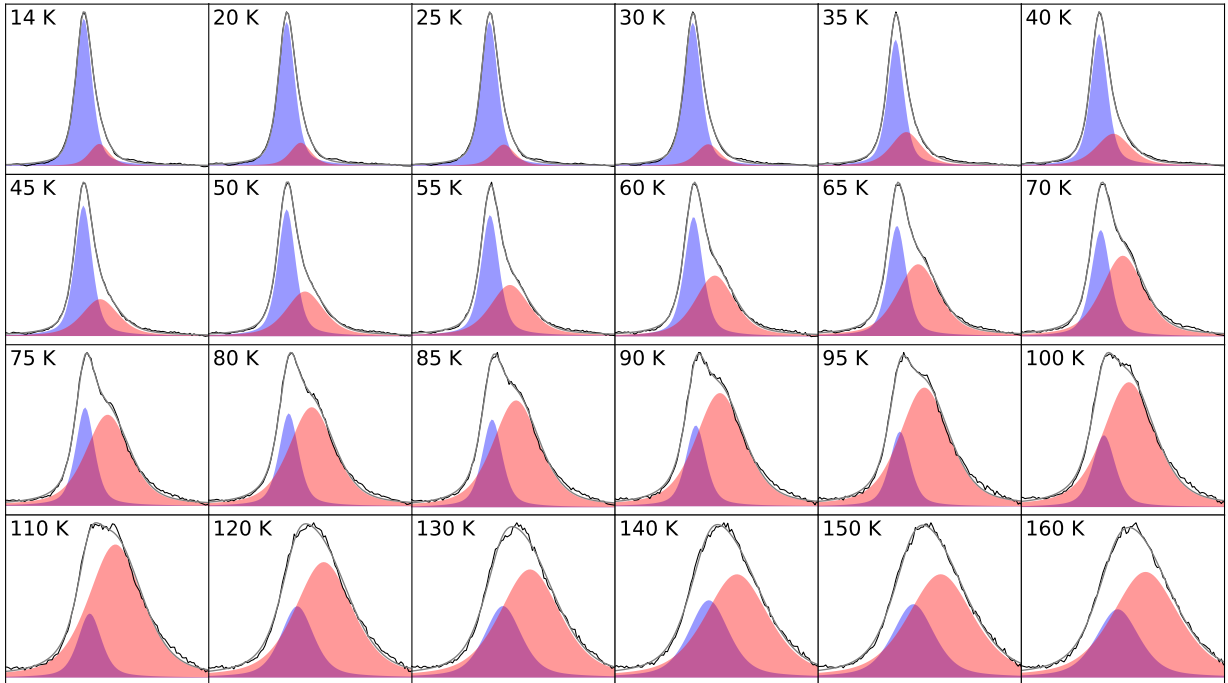
FIG. 4: Gaussian-Lorentzian fits of the $E_g^0 \rightarrow A_{1g}$ transition from 14 K to 160 K.

IV. CALCULATIONS OF CRYSTAL FIELD PARAMETERS AND PARAMETERS OF MAGNETO-ELASTIC COUPLING

Energies and wavefunctions of these levels can be found using the Stevens operator formalism, where the crystal field Hamiltonian takes the form

$$\mathcal{H}_{\mathrm{CEF}} = B_2^0 O_2^0 + B_4^0 O_4^0 + B_4^3 O_4^3 + B_6^0 O_6^0 + B_6^3 O_6^3 + B_6^6 O_6^6,$$

where O_n^m is the tensor operator and B_n^m is the crystal field parameter. In the framework of pure CEF excitations, it is reasonable to assume that the unperturbed E_g level takes the average energy of the double peaks. More precise values of the energies of the crystal field excitations obtained from Raman scattering spectra allows us to refine CEF parameters Table. II by fitting the CEF Hamiltonian with the starting values from the neutron scattering results[1]. The magnetoelastic interaction was diagonalized within the subspace spanned by the ground-state doublet with 0 phonon ($|\psi_1, 0\rangle, |\psi_2, 0\rangle$), the ground-state doublet with 1 phonon ($|\psi_1, \mu\rangle, |\psi_2, \mu\rangle$), and the doublet at 60 meV with 0 phonon ($|\psi_3, 0\rangle, |\psi_4, 0\rangle$). The magnetoelastic coupling constant was determined by the fitting of the observed splitting and turned out to be 0.07.

TABLE II: CEF parameters B_m^n (in µeV) for $Pr_2Zr_2O_7$ determined by Raman (this work) and Neutron scattering [1].

|	B_2^0	B_4^0	B_4^3	B_6^0	B_6^3	B_6^6
This work	-650.2	-33.08	-460.5	0.268	1.891	-1.987
Ref. [1]	-631	-32.36	-467.4	0.245	1.464	-1.907

TABLE III: Vibronic states of Pr^{3+} in the framework of magnetoelastic coupling.

E (meV)	$|\psi_1, 0\rangle$	$|\psi_2, 0\rangle$	$|\psi_1, \mu\rangle$	$|\psi_2, \mu\rangle$	$|\psi_3, 0\rangle$	$|\psi_4, 0\rangle$
57.18	0	0	0	0.712	-0.702	0
57.18	0	0	-0.712	0	0	-0.702
54.85	0	0	0	0.702	0.712	0
54.85	0	0	-0.702	0	0	0.712
0	1	0	0	0	0	0
0	0	1	0	0	0	0

TABLE IV: Pr^{3+} wave functions in the framework of pure CEF.

E (meV)	$\lvert-4\rangle$	$\lvert-3\rangle$	$\lvert-2\rangle$	$\lvert-1\rangle$	$\lvert0\rangle$	$\lvert1\rangle$	$\lvert2\rangle$	$\lvert3\rangle$	$\lvert4\rangle$
109.1	0	0.644	0	0	0.412	0	0	-0.644	0
94.38	0.128	0	0	0.306	0	0	-0.943	0	0
94.38	0	0	-0.943	0	0	-0.306	0	0	0.128
82.10	0	-0.707	0	0	0	0	0	-0.707	0
56.06	0.412	0	0	0.849	0	0	0.331	0	0
56.06	0	0	0.331	0	0	-0.849	0	0	0.412
9.24	0	-0.292	0	0	0.911	0	0	0.292	0
0	0	0	-0.017	0	0	0.431	0	0	0.902
0	-0.902	0	0	0.431	0	0	0.017	0	0

V. MAGNETIC SUSCEPTIBILITY
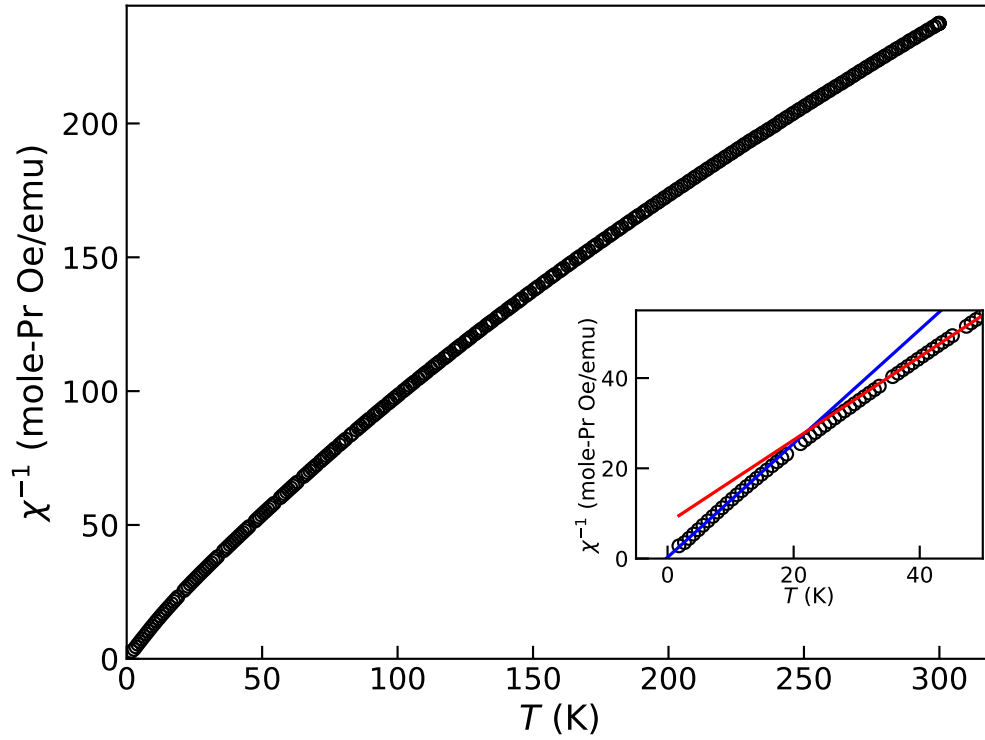
FIG. 5: Temperature dependence of the inverse DC magnetic susceptibility measured in the zero field cooling mode. Inset: linear regression fits for the data (i) from 2 to 10 K (blue line) and (ii) from 30 to 80 K (red line).

[1] P. Bonville, S. Guitteny, A. Gukasov, I. Mirebeau, S. Petit, C. Decorse, M. C. Hatnean, and G. Balakrishnan, Phys. Rev. B **94**, 134428 (2016).